Available online at www.sciencedirect.com
SCIENCE DIRECT®
Journal of Catalysis 224 (2004) 243–251
JOURNAL OF CATALYSIS
www.elsevier.com/locate/jcat

Inhibiting effect of H_2S on the DBT HDS activity of Ru-based catalysts—effect of the Cs addition

Atsushi Ishihara,* Jeayoung Lee, Franck Dumeignil, Masato Yamaguchi, Shigeki Hirao, Eika W. Qian, and Toshiaki Kabe

Department of Chemical Engineering, Tokyo University of Agriculture and Technology, Nakacho, Koganei, Tokyo 184-8588, Japan

Received 22 October 2003; revised 30 January 2004; accepted 24 February 2004

Available online 16 April 2004

Abstract

The effect of the Cs addition on the H_2S inhibition and subsequently on the DBT HDS activity over Ru-based catalysts was investigated. In good agreement with a previous study, the HDS activity over a Ru catalyst containing cesium was much higher than that over the same Ru catalyst without cesium. On the other hand, the HDS activity of the Ru–Cs catalyst was more inhibited by H_2S than that of the Ru catalyst at 260 °C. Thus, kinetic parameters were calculated using a Langmuir–Hinshelwood model to determine the mechanism of the H_2S inhibition over Ru and Ru–Cs catalysts. We found that the heats of adsorption of DBT and H_2S on the Ru–Cs catalyst were higher than on the Ru catalyst, indicating that the sulfur-containing species adsorb more strongly on the catalyst containing cesium. Subsequently, the role of cesium in the Ru–Cs catalyst on the DBT HDS activity was investigated by using ^{35}S-tracer experiments. The results suggested that while the Ru–Cs catalyst was more inhibited by H_2S, the Ru–S bonds were more stable on this catalyst than on the Ru catalyst. This Ru–S bond stabilization was responsible for the stabilization of the active phase, which allowed creation of a greater amount of sulfur atoms potentially labile. Thus, that explained the better HDS activity over the Ru–Cs catalyst than over the Ru catalyst, despite a greater H_2S inhibition on the former.

© 2004 Elsevier Inc. All rights reserved.

Keywords: Inhibiting effect of H_2S; Hydrodesulfurization; Dibenzothiophene; Ruthenium; Cesium; Sulfide; Alumina

1. Introduction

In recent years, due to more and more strict environmental regulations, much attention has been focused on the deep hydrodesulfurization (HDS) of light gas oils. From 1997, the maximum sulfur content in light gas oils has been limited to 500 ppm in most parts of the industrialized world. In addition, Japan decided recently to further reduce this maximal content to only 50 ppm until the year 2004. The European Union also recently proposed a reduction to only 50 ppm by the year 2005. Moreover, due to environmental considerations it will become necessary to lower these limitations further and further in the future. Thus, it is essential to develop novel highly efficient catalysts and to concomitantly elucidate the reaction mechanism under deep hydrodesulfurization reaction conditions. Among a large number of attempts, much attention has been focused on unsupported ruthenium sulfides, which were found to be the most active species in hydrodesulfurization of thiophenes using transition metal sulfides [1–5]. Actually, some of our recent studies aimed at optimizing ruthenium-based catalysts by different ways: investigation of the effect of the precursor [6]; addition of alkali [7]; and modification of the carrier [8]. These efforts permitted us to improve the HDS ability of the Ru sulfide-based catalysts. Especially, the alkali-promoted Ru catalysts (with Ru:Cs = 1:2) exhibited HDS activities comparable to that of a conventional Co–Mo catalyst [7]. Further, by the combined use of FTIR analysis and ^{35}S-tracer experiments, we found that in a Ru–Cs system (with Ru:Cs = 1:2) the Cs atoms strengthen the Ru–S bonds of the Ru sulfide species, with the consequence that S_0 (representing the amount of labile sulfur on the catalyst, assumed to be the number of active sites) increases and this increase was responsible for an increase in activity [9].

On the other hand, many research groups have reported that H_2S, which is a product of the HDS reaction, inhibits the

* Corresponding author. Fax: +81-42-388-7228.
E-mail address: atsushii@cc.tuat.ac.jp (A. Ishihara).

0021-9517/$ – see front matter © 2004 Elsevier Inc. All rights reserved.
doi:10.1016/j.jcat.2004.02.031

HDS reaction of organic sulfur compounds such as dibenzothiophene (DBT) and 4,6-dimethyldibenzothiophene (4,6-DMDBT) [10–14]. However, from our knowledge, the inhibiting effect of H_2S on the HDS of DBT using noble metal-based catalysts has been only scarcely studied. Thus, in the present work we investigated the inhibiting effect of H_2S on HDS of DBT over a Ru–carbonyl-based catalyst supported on alumina and a Ru–Cs-based catalyst supported on alumina. A Langmuir–Hinshelwood model for the reactions rates was applied in order to examine the kinetics of the H_2S inhibition. Further, the results were compared to the results obtained by ^{35}S-tracer experiments in order to give a more detailed picture of the DBT HDS reaction mechanism over Ru-based catalysts.

2. Experimental

2.1. Materials

Commercially available $Ru_3(CO)_{12}$ (Aldrich Co.), cesium hydroxide ($CsOH{\cdot}H_2O$), tetrahydrofuran (THF), decalin, and methanol (purity: 98%) (Kishida Chemicals) were used without further purification. DBT was supplied from Tokyo Kasei Industry Co., Ltd. Hydrogen and hydrogen sulfide (0–0.6 vol%) in hydrogen were supplied by Tohei Chemicals, γ-Al_2O_3 (specific surface area = 256 $m^2\,g^{-1}$; pore volume = 0.76 $cm^3\,g^{-1}$) was supplied by NIPPON Ketjen Co., Ltd.

2.2. Preparation of the catalysts

γ-Al_2O_3 was crushed and screened to obtain 20–30 mesh grains. The alumina was then dried under vacuum at 350 °C for 4 h and stored under an Ar atmosphere prior to use.

2.2.1. $Ru_3(CO)_{12}$–6CsOH/γ-Al_2O_3 catalyst (Ru:Cs = 1:2; Ru wt% = 8)

The $Ru_3(CO)_{12}$–6CsOH/γ-Al_2O_3 catalyst (Ru:Cs = 1:2) was prepared as follows: 0.1686 g of $Ru_3(CO)_{12}$, 0.2657 g of CsOH, H_2O, and 20 mL of methanol were introduced into a 50-mL reactor. After the mixture was stirred for 1 h, 0.9200 g of Al_2O_3 was added into the obtained solution, which was stirred for 2 h more. The solvent was removed under vacuum and the solid was stored under an Ar atmosphere prior to use. As a remark, while only a small amount of $Ru_3(CO)_{12}$ can be dissolved in methanol, CsOH is completely dissolved in this solvent and reacts easily with $Ru_3(CO)_{12}$ to give a $Cs^+[HRu_3(CO)_{11}]^-$ ruthenium anion carbonyl complex in a methanol solution that reacts further with the Lewis acid sites of the alumina.

2.2.2. $Ru_3(CO)_{12}$/γ-Al_2O_3 catalyst (Ru wt% = 8)

The $Ru_3(CO)_{12}$/γ-Al_2O_3 catalyst was prepared as follows: 0.1686 g of $Ru_3(CO)_{12}$ and 10 mL of THF were introduced into a 50-mL reactor. After the mixture was stirred for 1 h, 0.9200 g of Al_2O_3 was added into the obtained solution, which was stirred for 2 h more. The solvent was removed under vacuum and the catalyst was stored under an Ar atmosphere prior to use. Here, the solvent was chosen as THF because it dissolves $Ru_3(CO)_{12}$ unlike methanol. Therefore, it is used to dissolve and deposit the $Ru_3(CO)_{12}$ species on the Al_2O_3 surface without any destruction of its structure. Furthermore, these solvents used in the present research did not affect the HDS of DBT because they were entirely removed by vacuum when the catalysts were prepared.

2.3. Apparatus and procedure

The experimental apparatus was designed to work under high pressure. A fixed-bed flow reactor (stainless-steel tube with an internal diameter of 8 mm) was packed with 1.0 g of catalyst particles. The catalyst was presulfided using a mixture of 3 vol% H_2S in H_2 at 300 °C for 3 h. After the presulfidation, the reactor was cooled down in the H_2S/H_2 stream to the desired temperature and then the reactor was pressurized with hydrogen. The reactant solution was then introduced into the reactor by a high-pressure liquid pump (Kyowa Seimitsu KHD-16). The DBT HDS reaction was carried out under the following conditions: temperature, 240–320 °C; total pressure, 5 MPa; WHSV, 28 h^{-1}; flow rate of liquid, 32 mL/h; flow rate of H_2, 25 L/h; initial concentration of DBT, 0.1–1.0 wt%; H_2S partial pressure, 0–0.3 × 10^5 Pa. After steady state was reached (about 2 h), the first three samples of liquid products were collected from a gas–liquid separator every 15 min. The activity was taken as the mean value obtained for three samples. Then, the reaction temperature was increased and after a further stabilization time of 1 h and 30 min the next three samples were collected and analyzed. The same procedure was performed at each temperature. For each set of experiments (including the effect of H_2S) a back point was taken to check if any deactivation occurred. In any case the activity value calculated for the back point was the same as that of the initial point. The collected samples were analyzed by a gas chromatograph (Hitachi 163) equipped with a flame ionization detector and a G column 250 (i.d., 1.2 mm; film thickness, 1.0 μm; length, 40 m). The temperature of the column, the injector, and the detector were 210, 250, and 150 °C, respectively. The products were identified by GC-MS (QP2000/2000A).

2.4. Brief description of the kinetic models

The results of the DBT HDS reactions carried out under various H_2S concentrations were treated using appropriate kinetic equations. The selected model was the Langmuir–Hinshelwood kinetics that has been widely used for the HDS of DBT [15,16],

$$r_{\mathrm{HDS}} = \frac{k_{\mathrm{HDS}} K_{\mathrm{DBT}} P_{\mathrm{DBT}} K_{\mathrm{H_2}} P_{\mathrm{H_2}}}{(1 + K_{\mathrm{DBT}} P_{\mathrm{DBT}} + K_{\mathrm{H_2S}} P_{\mathrm{H_2S}})(1 + K_{\mathrm{H_2}} P_{\mathrm{H_2}})}, \quad (1)$$

where r_{HDS} is the rate of HDS; k_{HDS} is the rate constant of HDS; K_{DBT}, $K_{\mathrm{H_2S}}$, and $K_{\mathrm{H_2}}$ are the adsorption equilibrium

constants of DBT, hydrogen sulfide, and hydrogen, respectively; P_{DBT}, P_{H_2S}, and P_{H_2} are the partial pressures of DBT, hydrogen sulfide, and hydrogen, respectively.

According to the experimental conditions of the present study, Eq. (1) can be simplified. Indeed, as the hydrogen pressure is constant, the terms relative to hydrogen can be included in the rate constant. Based on the above assumption, Eq. (1) can be simplified into Eqs. (2) or (3):

$$r_{HDS} = \frac{k_{HDS} K_{DBT} P_{DBT}}{(1 + K_{DBT} P_{DBT} + K_{H_2S} P_{H_2S})}, \quad (2)$$

$$\frac{1}{r_{HDS}} = \frac{K_{H_2S} P_{H_2S}}{k_{HDS} K_{DBT} P_{DBT}} + \frac{(1 + K_{DBT} P_{DBT})}{k_{HDS} K_{DBT} P_{DBT}}. \quad (3)$$

In the case of the DBT HDS reactions performed without the addition of H_2S, the amount of H_2S formed was very small due to the low DBT concentration (0.1–1.0 wt%) under a high hydrogen pressure (5 MPa). Thus, the inhibition effect due to H_2S was not significant, and the retarding term $K_{H_2S} P_{H_2S}$ can be neglected. Based on the above assumption, Eq. (3) can be further simplified into Eq. (4):

$$\frac{1}{r_{HDS}} = \frac{1}{k_{HDS} K_{DBT} P_{DBT}} + \frac{1}{k_{HDS}}. \quad (4)$$

By plotting $1/r_{HDS}$ against $1/P_{DBT}$, k_{HDS}, and K_{DBT} can be calculated by determination of the relevant slope and intercept with the y axis.

3. Results

3.1. DBT HDS activity without addition of hydrogen sulfide

It has previously been found that ruthenium exhibits the highest HDS activity among unsupported transition metals [4]. Further, the HDS activity of alumina-supported ruthenium species could be increased by the addition of alkali metal [9]. In the present work, we decided to compare the H_2S inhibition over a Ru–alumina-based catalyst to the H_2S inhibition over the same catalyst containing Cs. First, DBT HDS reactions over the Ru/Al_2O_3 catalyst and the $Ru–Cs/Al_2O_3$ catalyst were performed without addition of hydrogen sulfide with various DBT concentrations to confirm the high HDS activity upon alkali addition (presented on Figs. 1 and 2). The conversion of DBT over both catalysts increased with increasing the temperature and decreasing the initial DBT concentration. The HDS activity of the Ru/Al_2O_3 catalyst was more influenced by the initial DBT concentration than the alkali-containing one. Moreover, while the DBT conversion of the Ru/Al_2O_3 catalyst was only about 37% at 320 °C in the case of the experiment performed with 1 wt% DBT, the $Ru–Cs/Al_2O_3$ catalyst exhibited an activity of about 88% for the same experimental conditions. Further, we presented the evolution of the fraction of DBT converted as a function of the DBT concentration in the feed for various experimental temperatures in Figs. 3 and 4. As shown in Fig. 3, the amount of DBT converted on Ru/Al_2O_3 exhibited an increase up to 0.4 wt% DBT in the feed but leveled off when the feed was more concentrated in DBT (except for the experiments performed at 320 °C for which a further slight increase in conversion was observed for 1 wt% DBT in the initial feed). In contrast, the amount of DBT converted on the $Ru–Cs/Al_2O_3$ catalyst increased linearly with the DBT concentration in the initial feed. This means that the surface activity sites present on the Ru/Al_2O_3 catalyst were saturated with DBT for a concentration of DBT of 0.4 wt% while they remained available in a sufficient quantity to perform the reaction on the $Ru–Cs/Al_2O_3$ catalyst even for a concentration of DBT of 1.0 wt%.

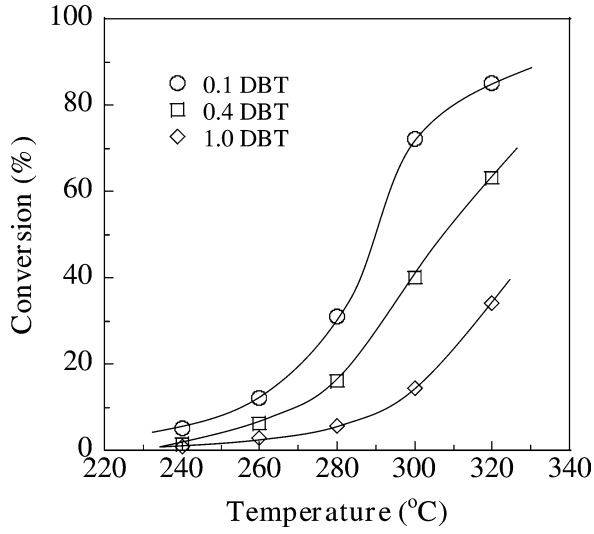

Fig. 1. Effect of the temperature on DBT conversion for various DBT concentrations (Ru/Al_2O_3 catalyst).

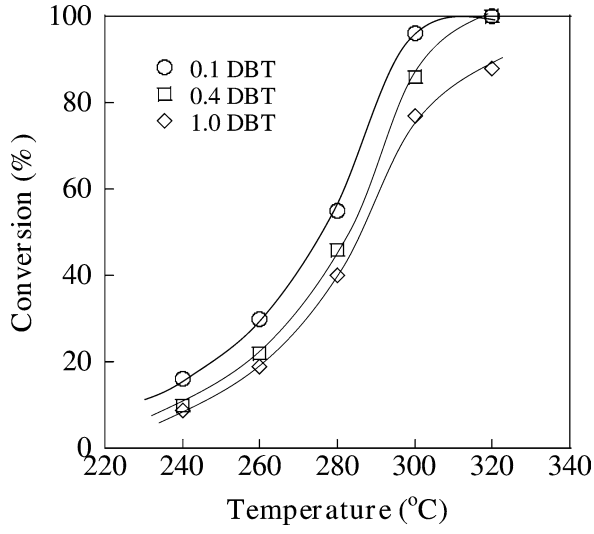

Fig. 2. Effect of the temperature on DBT conversion for various DBT concentrations ($Ru–Cs/Al_2O_3$ catalyst).

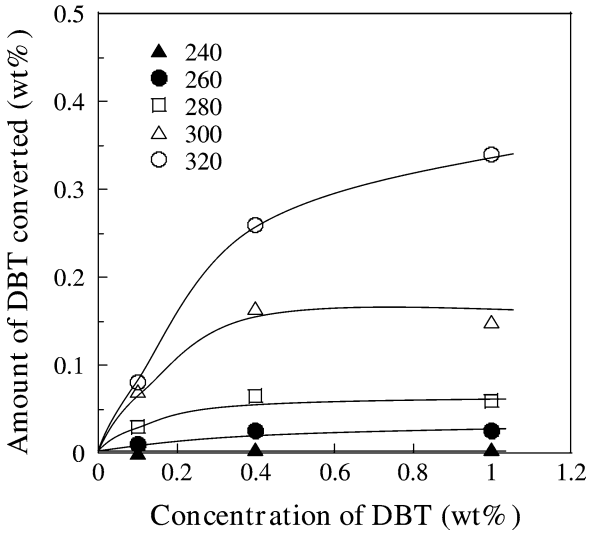

Fig. 3. Effect of the DBT concentration on the amount of DBT converted (Ru/Al_2O_3 catalyst).

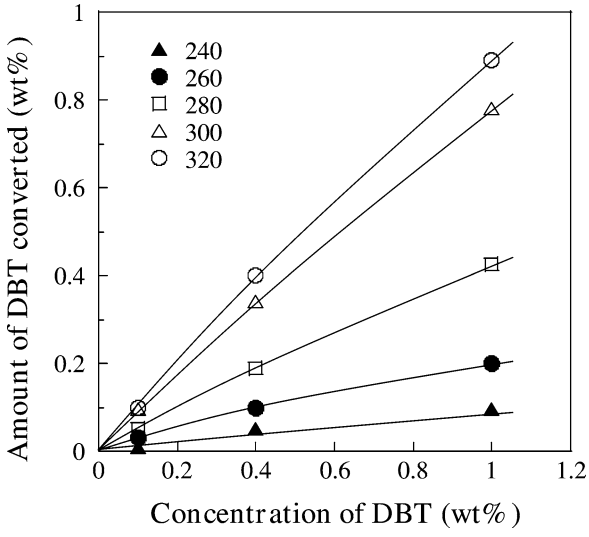

Fig. 4. Effect of the DBT concentration on the amount of DBT converted ($Ru–Cs/Al_2O_3$ catalyst).

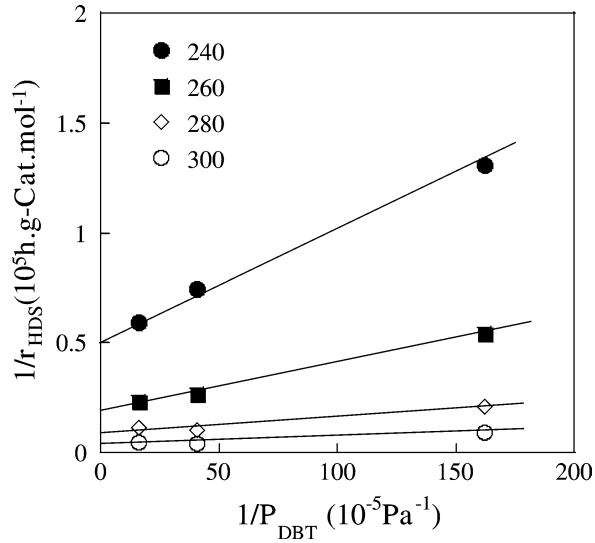

Fig. 5. $1/r_{HDS}$ as a function of $1/P_{DBT}$ (Ru/Al_2O_3 catalyst).

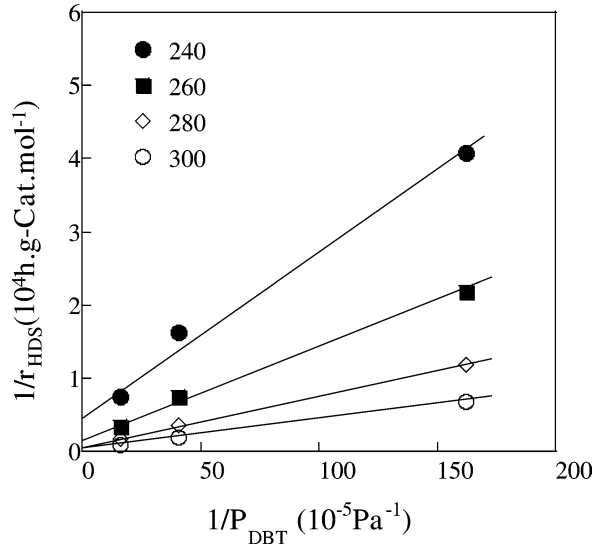

Fig. 6. $1/r_{HDS}$ as a function of $1/P_{DBT}$ ($Ru–Cs/Al_2O_3$ catalyst).

3.2. Results of the kinetic treatment

In order to examine whether Eq. (4) is actually adequate for the present study or not, we used it to treat our data. Figs. 5 and 6 show plots representing $1/r_{HDS}$ versus $1/P_{DBT}$ for the Ru/Al_2O_3 catalyst and the $Ru–Cs/Al_2O_3$ catalyst, respectively. The figures obtained for both catalysts exhibited a linear relationship, indicating that Eq. (4) could be reliably used for the present study. Thus, k_{HDS} and K_{DBT} were obtained upon determination of the slopes of the lines and the intercepts of the lines with the y axis.

Further, the DBT HDS was carried out while adding various concentrations of H_2S that were varied in the range from 0 to 0.51 vol% ($0–0.3 \times 10^5$ Pa). Eq. (3) was used to treat the obtained results. The obtained lines in Figs. 7 and 8 (for a DBT initial concentration of 1.0 wt%) exhibited linear relationships for the plots representing $1/r_{HDS}$ versus P_{H_2S} for both catalysts, indicating that Eq. (3) is adequate for the present study. K_{H_2S} could be estimated from the slopes after calculating k_{HDS} and K_{DBT} from Eq. (4).

3.3. Inhibiting effect of H_2S on the DBT hydrodesulfurization

To investigate the effect of H_2S on the DBT HDS rate over Ru/Al_2O_3 and $Ru–Cs/Al_2O_3$, HDS reactions were carried out under different H_2S partial pressures. Figs. 9 and 10 show the effects of the H_2S partial pressure on the DBT HDS rates over the Ru/Al_2O_3 catalyst and the $Ru–Cs/Al_2O_3$ catalyst, respectively. The HDS rates obtained over both catalysts decreased with increasing the H_2S partial pressure, which signifies that the addition of H_2S inhibited the DBT HDS reaction to a certain extent. As shown in Fig. 9, over

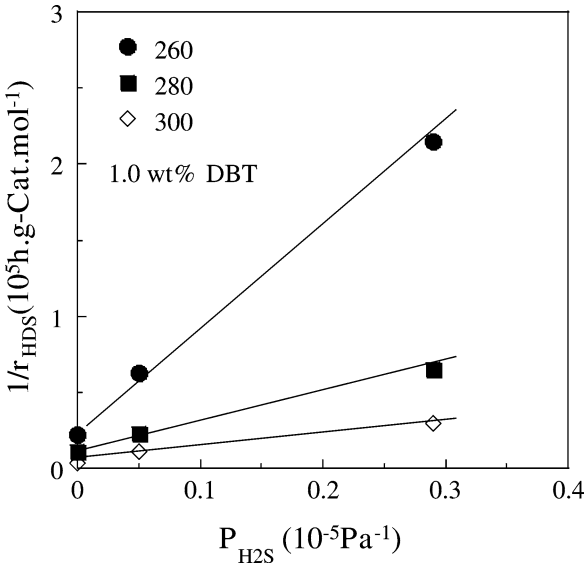

Fig. 7. $1/r_{HDS}$ as a function of $1/P_{H_2S}$ (Ru/Al_2O_3 catalyst).

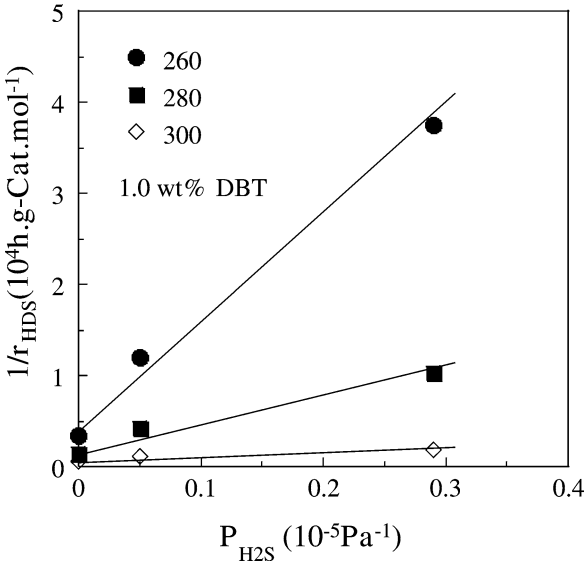

Fig. 8. $1/r_{HDS}$ as a function of $1/P_{H_2S}$ (Ru–Cs/Al_2O_3 catalyst).

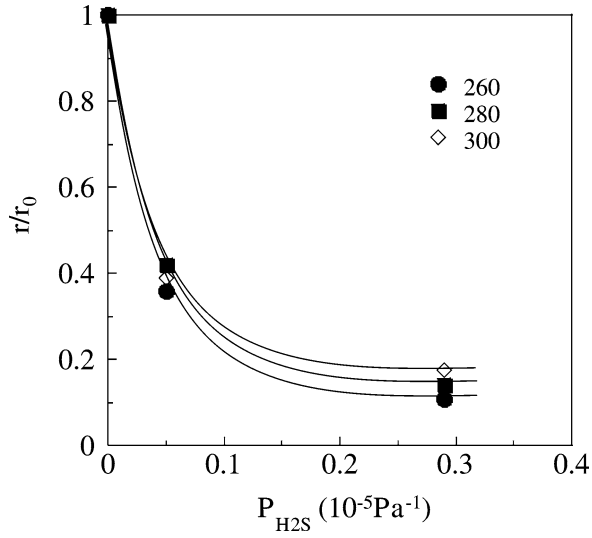

Fig. 9. Effect of the H_2S partial pressure on DBT HDS activity (Ru/Al_2O_3 catalyst, 1.0 wt% DBT).

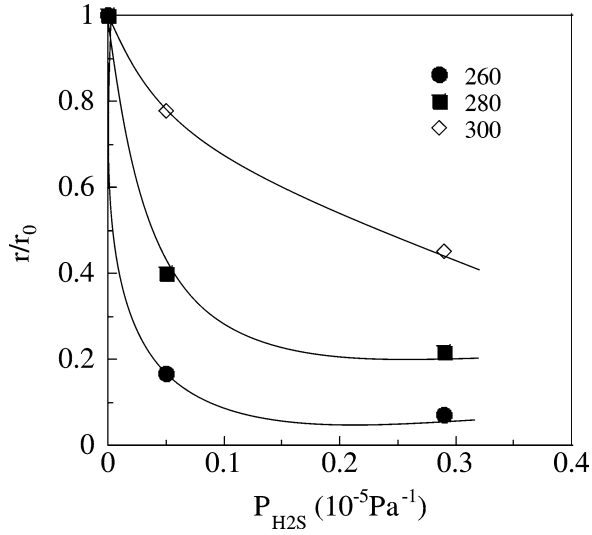

Fig. 10. Effect of the H_2S partial pressure on DBT HDS activity (Ru–Cs/Al_2O_3 catalyst, 1.0 wt% DBT).

the Ru/Al_2O_3 catalyst the DBT HDS rate under a H_2S partial pressure of 0.05×10^5 Pa decreased about 65% when compared to the rate obtained without addition of H_2S at 260 °C. In contrast, using the Ru–Cs/Al_2O_3 catalyst, the DBT HDS rate under a H_2S partial pressure of 0.05×10^5 Pa decreased about 80% when compared to the rate obtained without addition of H_2S at 260 °C. These results show that the DBT HDS over the Ru–Cs/Al_2O_3 catalyst was more strongly inhibited by H_2S than over the Ru/Al_2O_3 catalyst. Moreover, while the inhibiting degree of H_2S over the Ru/Al_2O_3 catalyst was quite independent of the temperature, that observed over the Ru–Cs/Al_2O_3 catalyst became lower with increasing temperature (Figs. 9 and 10). This implies that the absolute value of the adsorption equilibrium constant between DBT and H_2S on the Ru–Cs/Al_2O_3 catalyst was more influenced by an increase in temperature than the Ru/Al_2O_3 catalyst.

In addition, for a comparison of the inhibiting effects of H_2S between different types of catalysts, some results that we previously obtained over Mo and CoMo catalysts [17,18] are reported in Fig. 11 together with the results obtained in the present study over the Ru catalyst and the Ru–Cs catalyst. Thus, Fig. 11 shows the effect of H_2S on the HDS reaction of DBT over various catalysts at reaction temperatures of 260 °C. The results clearly indicate that the inhibiting effect of H_2S on the DBT HDS over various catalysts increased in the order Ru < Ru–Cs ⩽ Co–Mo < Mo at 260 °C.

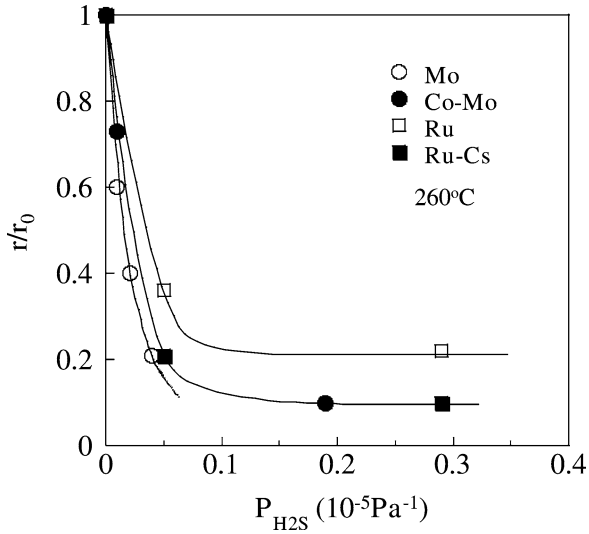

Fig. 11. Effect of the H_2S partial pressure on DBT HDS activity (alumina-supported Mo, Co–Mo, Ru, and Ru–Cs catalysts).

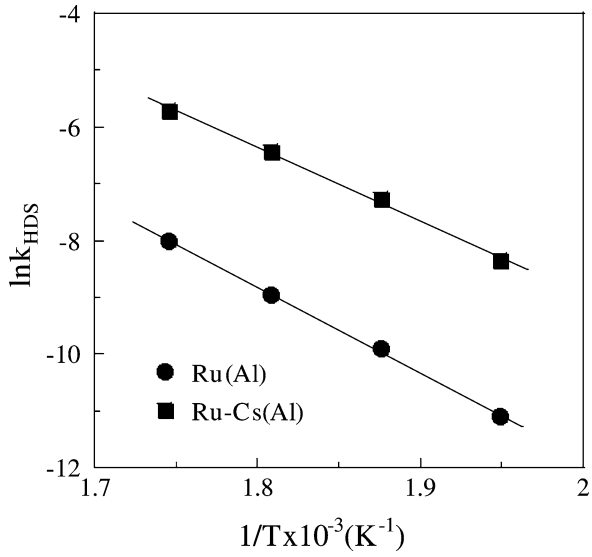

Fig. 12. Arrhenius plots.

3.4. Arrhenius and Van't Hoff plots

To elucidate the mechanism of the inhibiting effect of H_2S on the HDS activity over Ru and Ru–Cs catalysts, we estimated the activation energy of the HDS reaction from the activity results and subsequently calculated the heats of adsorption of DBT and H_2S using the Langmuir–Hinshelwood model (see the details in Section 2). The rate constants of HDS (k_{HDS}) and the adsorption equilibrium constant of DBT (K_{DBT}) were calculated using Eq. (4), while the adsorption equilibrium constant of hydrogen sulfide (K_{H_2S}) was calculated using Eq. (3). Fig. 12 shows the Arrhenius plots for the DBT HDS reaction over Ru and Ru–Cs catalysts. The activation energy calculated from the slopes for the Ru and the Ru–Cs catalyst were 126 and 109 kJ/mol, respectively. Then, Figs. 13 and 14 show the Van't Hoff plots for the DBT HDS over Ru and Ru–Cs catalysts, respectively. The heats of adsorption calculated from the slope of each line are summarized in Table 1. The heats of adsorption of DBT and H_2S on the Ru/Al_2O_3 catalyst were 13 and 29 kJ/mol, respectively, while the heats of adsorption of DBT and H_2S on the $Ru–Cs/Al_2O_3$ catalyst were 38 and 126 kJ/mol, respectively. While the value of the activation energy reflects the relative difficulty of the desulfurization of DBT, the values of the heat of adsorption reflect the relative strength of the adsorption of DBT or H_2S on the catalysts. Considering this, from the values of the heat of adsorption of DBT and H_2S over Ru and Ru–Cs catalysts, it seems that in both cases the adsorption of H_2S on the catalysts is stronger than DBT, which means that the DBT HDS is hindered to a certain extent. In particular, the heats of adsorption of DBT and H_2S were higher on the $Ru–Cs/Al_2O_3$ catalyst than on the Ru/Al_2O_3 catalyst, suggesting that the addition of cesium to Ru/Al_2O_3 catalysts makes easier the adsorption of sulfur on the surface of said catalysts.

Table 1
Results of the kinetic treatments for various catalysts

Catalysts	Conversion[a]	E_a[b]	Q_{DBT}[c]	Q_{H_2S}[d]	S_0[e]	k_{RE}[f]	NO[g]
Ru	14	126	13	29	4.2	2.6	130
Ru–Cs	74	109	38	126	31	1.9	910
Mo	22	105	42	88	13	1.4	110
Co–Mo	92	105	42	71	26	2.9	260

[a] DBT conversion (%) at 300 °C for 1 wt% of DBT.
[b] HDS activation energy (kJ/mol).
[c] DBT heat of adsorption (kJ/mol).
[d] H_2S heat of adsorption (kJ/mol).
[e] Labile sulfur quantity (mg_S/g_{cat}).
[f] H_2S release rate constant (10^{-2} min^{-1}).
[g] NO adsorption ($\mu mol/g_{cat}$).

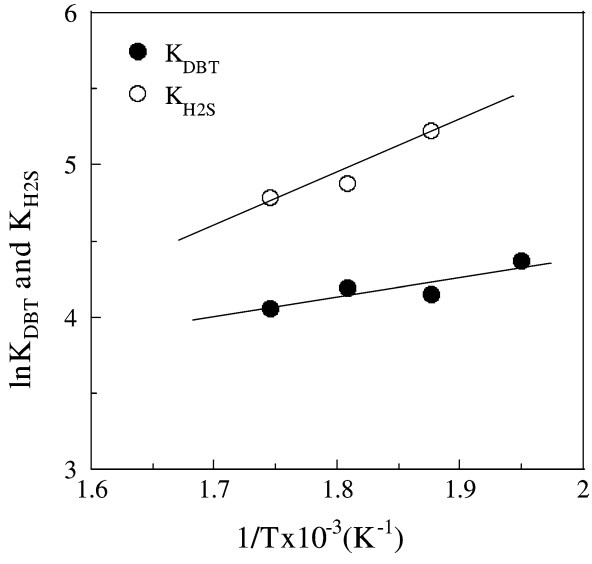

Fig. 13. Van't Hoff plots for the DBT and the H_2S adsorption equilibrium constants (Ru/Al_2O_3 catalyst).

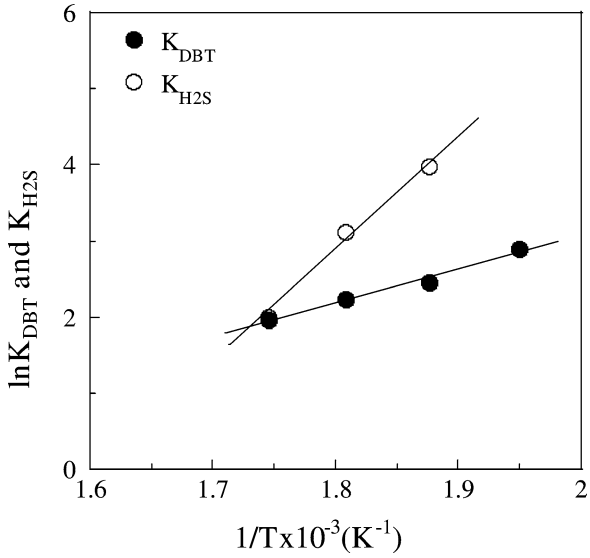

Fig. 14. Van't Hoff plots for the DBT and the H_2S adsorption equilibrium constants (Ru–Cs/Al_2O_3 catalyst).

4. Discussion

In a previous study, from FT-IR results [7] we showed that when $Ru_3(CO)_{12}$ was treated with sixfold CsOH in methanol, all the $Ru_3(CO)_{12}$ species were converted into Cs-[$HRu_3(CO)_{11}$]. Further, after the Cs[$HRu_3(CO)_{11}$] species were supported on alumina, they were stabilized for Cs/Ru $\geqslant 2$. Then, the experimental results showed that the preservation of the formed anionic species on the alumina (effective consequently to their stabilization for Cs/Ru $\geqslant 2$) as well as the proximity of the Cs and the Ru species permitted the increase in the HDS activity. In the present study, the Ru–Cs/Al_2O_3 catalyst (with Cs/Ru = 2) exhibited effectively a HDS activity higher than that of the Ru/Al_2O_3 catalyst.

Figs. 3 and 4 showed that the amount of DBT converted over the Ru/Al_2O_3 catalyst increased with increasing the DBT concentration up to 0.4 wt% DBT for which it stabilized (only for 320 °C, further increase in DBT concentration up to 1 wt% led to a slight increase in conversion). In contrast, the amount of DBT converted over the Ru–Cs/Al_2O_3 catalyst increased linearly up to 1 wt%. Further, we reported the amount of NO chemisorption over Ru/Al_2O_3 and Ru–Cs/Al_2O_3 catalyst [7] in Table 1 with the data obtained for Mo/Al_2O_3 and Co–Mo/Al_2O_3 catalysts [19,20]. Indeed, the amount of coordinatively unsaturated sites (CUS) on a catalyst is often related to the catalytic activity and can be estimated, for instance, by NO chemisorption. In the aforementioned NO chemisorption experiments, the quantity of Ru and Mo was about the same (about 7.9×10^2 μmol) and all the catalysts were presulfided (at 300 °C, 3 h for the Ru/Al_2O_3 and the Ru–Cs/Al_2O_3 catalysts and at 400 °C, 3 h for the Mo/Al_2O_3 and the Co–Mo/Al_2O_3 catalysts, respectively). As shown in Table 1, the amount of NO chemisorbed on the Ru–Cs/Al_2O_3 catalyst was much higher (7 times) than that on the Ru/Al_2O_3 catalyst. This result explains why the amount of DBT converted on the Ru–Cs/Al_2O_3 catalyst increased up to 1 wt% DBT contrary to the Ru/Al_2O_3 for which stabilization was observed for 0.4 wt% DBT. However, as shown in Fig. 11, at 260 °C the value of r/r_0 for the Ru–Cs/Al_2O_3 catalyst decreased more rapidly than for the Ru/Al_2O_3 catalyst with increasing the H_2S partial pressure, indicating that the Ru–Cs/Al_2O_3 catalyst was more inhibited by H_2S than the Ru/Al_2O_3 catalyst. In order to explain this phenomenon, some kinetic parameters were determined. We found that the heat of adsorption of H_2S calculated from the Langmuir–Hinshelwood equation was larger than that of DBT on both catalysts (Table 1). This indicates that H_2S was adsorbed more strongly on the catalysts than DBT and thus inhibited the DBT HDS reaction through competitive adsorption. In addition, the heats of adsorption of H_2S and DBT on the Ru–Cs/Al_2O_3 catalyst were higher than on the Ru/Al_2O_3 catalyst. This means that the sulfur species were more strongly adsorbed on the Ru–Cs catalyst than on the Ru catalyst.

To have an idea of the sulfide state of each catalyst during HDS working conditions, the results of ^{35}S-tracer experiments were also given in Table 1 and then compared with the kinetic data. Here, S_0, the amount of labile sulfur on each catalyst, means the amount of active sites and k_{RE}, the [^{35}S]H_2S release rate constant, indicates the relative ease of migration of the sulfur from the catalyst. While the release rate constant of H_2S on the Ru/Al_2O_3 catalyst was higher than on the Ru–Cs/Al_2O_3 catalyst, the amount of labile sulfur on the Ru–Cs/Al_2O_3 catalyst was much higher than that on the Ru/Al_2O_3 catalyst. These results suggest that while the addition of cesium to the Ru/Al_2O_3 catalyst decreases the lability of the active sites, it increases their amount. The fact that the S species are more strongly adsorbed on the Ru–Cs catalyst and that a greater number of active sites is present allows us to negate that these Ru–Cs catalysts undergo a reduction into the Ru metallic form. When Cs is not present, due to the large quantities of H_2 in the reactor, the RuS_2 active phase is unstable and can be partially reduced into metallic Ru, which is not favorable for the activity. When adding Cs, the "RuS" active phase is stabilized through an increase in the RuS bond strength, and therefore the existence of the active sites is preserved. Further, the strengthening of the RuS bond indicates that the velocity of cleavage of the DBT C–S bond increases and therefore, the HDS activity of the Ru–Cs/Al_2O_3 catalyst globally increases to give a performance better than that of the Ru/Al_2O_3 catalyst.

For comparison, the values obtained for Mo and Co–Mo catalysts are also shown in Table 1. No significant difference in the heat of adsorption of DBT or H_2S [17,18] was observed between the Mo and the Co–Mo catalyst. Nevertheless, both the amount of labile sulfur and the release rate constant of H_2S on the Co–Mo catalyst [21,22] were higher than on the Mo catalyst, explaining the higher activity of the Co–Mo catalyst. In other words, while the promoter Co in-

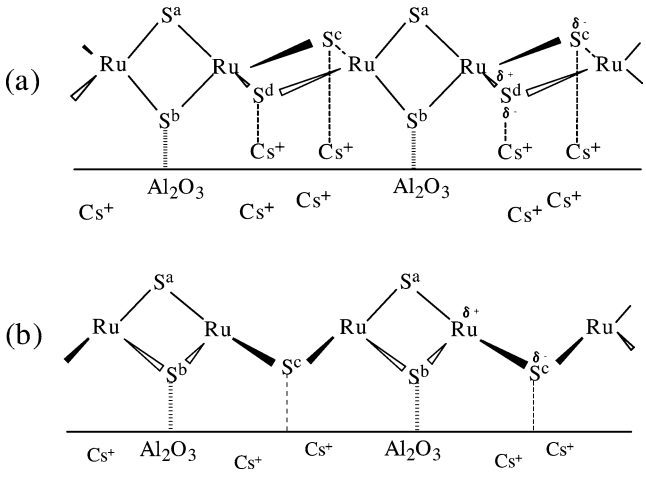

Fig. 15. Sulfided Ru–Cs/Al_2O_3 catalyst structure. (a) RuS_2; (b) $RuS_{1.5}$.

duces an increase in the active site numbers as well as an increase in the reactivity of the active sites of Mo-based catalysts, the beneficial effect of the addition of Cs to Ru/Al_2O_3 catalysts is of a different type as the reactivity of the active sites is decreased and their number increases.

Further, we previously reported the structure of the active phase on sulfided Ru–Cs/Al_2O_3 catalysts [9,23] (Fig. 15). For the catalysts with Cs/Ru ratios superior to 2 or 3 (Fig. 15a) the interaction between Cs and Ru strengthens the Ru–S bond [9] and thus three types of sulfur species can be distinguished as represented in Fig. 15a. The sulfur present between the ruthenium layer and the alumina surface (S^b) might be the most difficult to move while the sulfur over the ruthenium layer (S^a) might be the most labile. Two sulfurs in other position (S^c and S^d), which form triangles parallel to the alumina surface together with Ru, may have an average lability. In contrast, for the catalysts with Cs/Ru = 1, the RuCs complex is destroyed after impregnation [7], and the structure of the catalysts is very likely to be like the one in Fig. 15b. Indeed, in this case all the introduced Cs is consumed to neutralize the alumina acid sites and most of them are located in the alumina matrix. Furthermore, the results from NO chemisorption, the value of S_0 (Table 1), and Fig. 3 indicate that the Ru dispersion on the Ru/Al_2O_3 catalyst (Cs/Ru = 0) is like to be quite low. That means that the Ru/Al_2O_3 catalyst is certainly sintered during the sulfidation procedure. In brief, these results show that the addition of adequate quantities of cesium to the Ru/Al_2O_3 catalyst strengthens the Ru–S bonds and thus the sulfur species S^a, S^b, S^c, and S^d of Fig. 15a are preserved. As a consequence, a greater amount of labile sulfur (S_0) can be potentially created with a high dispersion of Ru on the Cs-promoted Ru/Al_2O_3 catalysts. Indeed, the addition of an adequate quantity of cesium to the Ru/Al_2O_3 catalyst allows not only an increase of the Ru dispersion on the catalyst but also a promotion of the C–S bond cleavage while stabilizing the Ru–S bonds and consequently the active phase by avoiding its overreduction when the catalyst is placed under

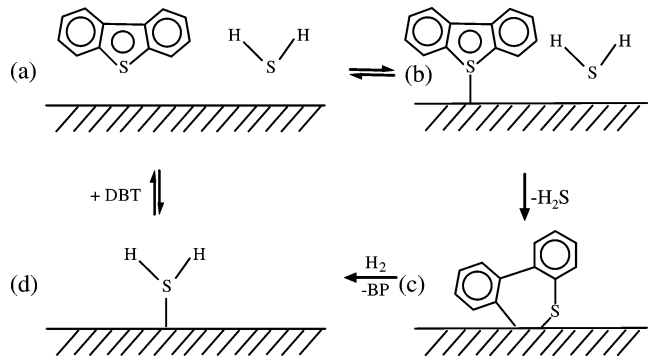

Fig. 16. Mechanism on hydrodesulfurization catalyzed by alumina-supported ruthenium system catalysts.

HDS working conditions. This explains why a higher HDS activity was obtained on the Ru–Cs/Al_2O_3 catalyst.

Then, the mechanism of the DBT hydrodesulfurization over alumina-supported ruthenium-based catalysts is proposed (Fig. 16). In the HDS working conditions, the possible adsorption/desorption states of the sulfur species are represented in Figs. 16a to 16d. At the steady state, DBT and the produced H_2S are both present in the system (Fig. 16a). Then, DBT can adsorb on an active site and a kind of metallathiabenzene is formed (as represented in Fig. 16c). Further, the metallathiabenzene reacts with hydrogen to produce biphenyl (Fig. 16d) and HDS is performed on free active sites according to the proposed cycle. For a Ru catalyst, the heats of absorption of H_2S and DBT were smaller than the ones observed over the Ru–Cs catalyst, indicating a relatively weak sulfur adsorption. Nevertheless, some DBT molecules can be adsorbed on the Ru catalyst surface as shown in Fig. 16b and the reaction can further proceed in the same matter as the one proposed in Figs. 16c and 16d. In addition, the active sites number was lower than over the Ru–Cs catalyst. Thus, in the case of the Ru catalyst, the states represented in Figs. 16a or 16b may become predominant under the HDS working conditions (weak adsorption + low quantity of active sites). In contrast, for a Ru–Cs catalyst, the heats of absorption were higher than those observed over the Ru catalyst, indicating a relatively strong sulfur adsorption state. Further, the results of NO chemisorption and ^{35}S-tracer experiments indicated a high dispersion of the Ru species on the Ru–Cs catalyst and the active sites were stable even under a pressurized hydrogen atmosphere. Accordingly, for the Ru–Cs catalyst, the steady state under HDS working conditions might be of the type of that given in Figs. 16c or 16d. Taking in consideration the above results, the reaction pathway from (d) to (a) supposedly progresses faster on the Ru catalyst (high k_{RE} and low adsorptions heats that suggest easy desorption of the products) than on the Ru–Cs catalyst but, as the number of active sites is higher on the Ru–Cs catalyst, the reaction pathway from (b) to (c) progresses faster on the Ru–Cs catalyst and thus the global amount of converted molecules is higher. In brief, while the H_2S poisoning is lower on the Ru catalyst, the number of

active sites is also lower and the activity is therefore lower than the one observed over a Ru–Cs catalyst. Indeed, this latter exhibits a large number of active sites, which is sufficient to compensate the larger H_2S hindrance.

In brief, the present kinetic results were in good agreement with the results of previous studies, while permitting a more detailed picture of the working Ru and Ru–Cs catalysts.

5. Conclusions

The activity of a catalyst derived from the alumina-supported $Ru_3(CO)_{12}$–alkali metal hydroxide complex was compared with that of a catalyst derived from $Ru_3(CO)_{12}$. As observed in a previous study, we confirmed that the addition of an alkali (here Cs) remarkably promoted the HDS activity of a ruthenium catalyst. Then, the effect of H_2S on the catalytic activity was investigated. The HDS rates of both Ru and Ru–Cs catalysts decreased with increasing the partial pressure of H_2S. In particular, the Ru–Cs/Al_2O_3 catalyst was more inhibited by H_2S than Ru/Al_2O_3 catalysts at 260 °C. Thus, some important kinetic parameters were calculated using the Langmuir–Hinshelwood equations. We found that the heat of adsorption of H_2S was larger than that of DBT on both catalysts, indicating that H_2S was adsorbed on the catalyst more strongly than DBT with the consequence of inhibiting the DBT HDS to a certain extent. Especially, the heats of adsorption of DBT and H_2S on the Ru–Cs catalyst were quite high (38 and 126 kJ/mol, respectively) compared with the Ru catalyst (13 and 29 kJ/mol, respectively), indicating that sulfur species adsorb on the catalyst more easily upon cesium addition. The role of the cesium in the Ru–Cs catalyst for DBT HDS was examined using the results of ^{35}S-tracer experiments. It showed that while the cesium-containing Ru catalyst was more inhibited by H_2S, the Ru–S bonds were stabilized supposedly by the presence of Cs atoms in their vicinity, as previous FT-IR results suggested. Consequently, the amount of labile sulfur increased sufficiently on the Ru–Cs/Al_2O_3 catalyst to overcome the enhanced H_2S hindering, which finally led to a global increase in the HDS activity.

References

[1] M. Vrinat, M. Lacroix, M. Breysse, L. Mosoni, M. Roubin, Catal. Lett. 3 (1989) 405.
[2] A.P. Raje, S.-J. Liaw, B.H. Davis, Appl. Catal. 150 (1997) 297.
[3] A.P. Raje, S.-J. Liaw, R. Srinivasan, B.H. Davis, Appl. Catal. 150 (1997) 319.
[4] T.A. Pecoraro, R.R. Chianelli, J. Catal. 67 (1981) 430.
[5] M. Lacroix, N. Boutarfa, C. Guillard, M. Vrinat, M. Breysse, J. Catal. 120 (1989) 473.
[6] A. Ishihara, M. Nomura, T. Kabe, J. Jpn. Petrol. Inst. 37 (1994) 300.
[7] A. Ishihara, M. Nomura, N. Takahama, K. Hamaguchi, T. Kabe, J. Jpn. Petrol. Inst. 39 (1996) 211.
[8] A. Ishihara, M. Nomura, K. Shirouchi, T. Kabe, J. Jpn. Petrol. Inst. 39 (1996) 403.
[9] A. Ishihara, J. Lee, F. Dumeignil, R. Higashi, A. Wang, E.W. Qian, T. Kabe, J. Catal. 217 (2003) 59.
[10] H. Gissy, R. Bartsch, C. Tanielin, J. Catal. 65 (1980) 158.
[11] M. Yamada, Y.L. Shi, T. Obara, K. Sakaguchi, Sekiyu Gakkaishi 33 (1990) 227.
[12] D.H. Broderick, E.C. Gates, AIChE J. 27 (1981) 663.
[13] G.H. Singhal, R.L. Espino, J.E. Sobel, G.A. Huff Jr., J. Catal. 67 (1981) 457.
[14] T. Kabe, Y. Aoyama, D. Wang, A. Ishihara, W. Qian, M. Hosoya, Q. Zhang, Appl. Catal. A 209 (2001) 237.
[15] M.L. Vrinat, Appl. Catal. 6 (1983) 137.
[16] T.C. Ho, J.E. Sobel, J. Catal. 128 (1991) 581.
[17] Q. Zhang, W. Qian, A. Ishihara, T. Kabe, Sekiyu Gakkaishi 40 (1997) 429.
[18] T. Kabe, W. Qian, A. Ishihara, Catal. Today 39 (1997) 3.
[19] A. Ishihara, M. Azuma, M. Matsushita, T. Kabe, Sekiyu Gakkaishi 36 (1996) 360.
[20] A. Ishihara, M. Matsushita, K. Shirouchi, Q. Zhang, T. Kabe, Sekiyu Gakkaishi 39 (1996) 26.
[21] T. Kabe, W. Qian, S. Ogawa, A. Ishihara, J. Catal. 143 (1993) 239.
[22] T. Kabe, W. Qian, A. Ishihara, J. Catal. 149 (1994) 171.
[23] A. Ishihara, M. Yamaguchi, H. Godo, W. Qian, M. Godo, T. Kabe, Sekiyu Gakkaishi 41 (1998) 51.